Skin Research and Technology 2013; **19**: 194–204
Printed in Singapore · All rights reserved
doi: 10.1111/srt.12035

Published by Blackwell Publishing Ltd
Skin Research and Technology

High resolution diagnosis of common nevi by multiphoton laser tomography and fluorescence lifetime imaging

Federica Arginelli[1], Marco Manfredini[1], Sara Bassoli[1], Christopher Dunsby[2], Paul French[2], Karsten König[3,4], Cristina Magnoni[1], Giovanni Ponti[1,5], Clifford Talbot[2] and Stefania Seidenari[1]

[1]*Department of Dermatology, University of Modena and Reggio Emilia, Modena, Italy,*
[2]*Department of Physics, South Kensington Campus, Imperial College London, London, UK,*
[3]*Department of Biophotonics and Lasertechnology, Saarland University, Saarbrücken, Germany,*
[4]*JenLab GmbH, Jena, Germany and* [5]*Department of Clinical and Diagnostic Medicine and Public Health, University Hospital of Modena and Reggio Emilia, Italy*

Background: Multiphoton Laser Tomography (MPT) has developed as a non-invasive tool that allows real-time observation of the skin with subcellular resolution. MPT is readily combined with time resolved detectors to achieve fluorescence lifetime imaging (FLIM). The aim of our study was to identify morphologic MPT/FLIM descriptors of melanocytic nevi, referring to cellular and architectural features.

Methods: In the preliminary study, MPT/FLIM images referring to 16 ex vivo nevi were simultaneously evaluated by 3 observers for the identification of morphologic descriptors characteristic of melanocytic nevi. Proposed descriptors were discussed and the parameters referring to epidermal keratinocytes, epidermal melanocytes, dermo-epidermal junction, papillary dermis and overall architecture were selected. In the main study, the presence/absence of the specified criteria were blindly evaluated on a test set, comprising 102 ex vivo samples (51 melanocytic nevi, 51 miscellaneous skin lesions) by 2 observers.

Results: Twelve descriptors were identified: "short-lifetime cells in the stratum corneum", "melanin-containing keratinocytes", "dendritic cells", "small short-lifetime cells" in the upper and lower layers", "edged papillae", "non-edged papillae", "junctional nests of short-lifetime cells", "dermal cell clusters", "short-lifetime cells in the papilla", "monomorphic and regular histoarchitecture", "architectural disarray".

Conclusion: Identified descriptors for benign melanocytic lesions proved sensitive and specific, enabling the differentiation between melanocytic nevi and non-melanocytic lesions.

Key words: multiphoton laser tomography – fluorescence lifetime imaging – melanocytic nevi, diagnosis – reflectance confocal microscopy – melanin

Accepted for publication 10 November 2012

COMMON NEVI are a wide group of benign lesions including entities histologically characterized by an increased number and proliferation of typical melanocytes, in single cells or in aggregates, where they tend to assume an epithelioid configuration. From a histological point of view, we differentiate junctional, compound and intradermal nevi. Junctional nevi are characterized by a proliferation of single cells at the junction (jentigo type) or small junctional nests. The compound nevus subtype has a junctional and a dermal component which can involve the superficial or the deep dermis, whereas intradermal nevi include nevi with nests only localized in the dermis.

Clinically, nevi can be distinguished for their presentation as flat, palpable, or frankly dome-shaped lesions, according to the dermal involvement. In fact, a junctional nevus tends to be totally flat, but while dermal nests start to deepen in the upper dermis, it may become palpable. As the nests reach the deep dermis, the elevation of the nevus occurs, conferring the papulous aspect typical of dermal nevi.

Nevi are clinically relevant because they may look very similar to malignant melanocytic lesions. Early diagnosis of melanoma represents the only means to defeat this potentially lethal tumour with certainty. The differential diagnosis between a common nevus and a melanoma

is usually performed by clinical and instrumental examinations. Since clinical assessment alone does not achieve a satisfactory identification of suspicious lesions (1), non-invasive imaging techniques such as dermoscopy and reflectance confocal microscopy (RCM) have been introduced to enable the clinician both to early detect melanoma and to avoid unnecessary surgical removals (2–4).

Under dermoscopy, junctional nevi usually show a reticular pattern, with brown to black regular meshes surrounding lighter holes; the corresponding feature in RCM is the ringed pattern, with regular edged papillae formed by regularly sized and shaped bright cells, surrounding dark oval spaces (dermal papillae) (5).

Compound nevi are characterized by a reticular-globular or reticular-globular-homogeneous pattern in dermoscopy, while RCM features include a meshwork pattern, with abundant junctional and dermal nests. A clod pattern is observable when the aggregation in nests of melanocytic cells is prevalent (6).

Dermal nevi are featured in dermoscopy by a cobblestone pattern, with light to dark, polygonal to roundish globules on a homogeneously pigmented area. Under RCM the epidermal and junctional layers are thinned due to the dermal expansion of melanocytes, and the most commonly seen feature includes the presence of homogeneous dense nests expanding the dermal papillae (7).

Recently, multiphoton laser tomography (MPT) has developed as a new non-invasive tool that allows real-time observation of the skin with subcellular resolution. This nonlinear optical technique employs a near-infrared (NIR) ultrafast laser (femtosecond pulses) to achieve an efficient nonlinear excitation of fluorophores and a penetration depth of 200 μm (8–10). MPT is readily combined with time resolved detectors to achieve fluorescence lifetime imaging (FLIM).

Multiphoton laser tomography and MPT-FLIM have been extensively employed for the definition of basal cell carcinoma (BCC) features *in vivo* and *ex vivo*, with the identification of specific basal cell carcinoma descriptors, enabling its differentiation from healthy skin and from other skin lesions (11–15).

So far, only two MPT studies focused on the features of melanocytic lesions. Investigating autofluorescent images (MPT images without FLIM) of 83 melanocytic lesions, Dimitrow et al. assessed the potential of this technique for the determination of the sensitivity and the specificity for the diagnosis of malignant melanoma (16). In a second study carried out by the same group also employing FLIM, a significant difference in the lifetime behaviour of keratinocytes in comparison to melanocytes was demonstrated (17).

The aim of our study was to identify morphological descriptors of melanocytic nevi, referring both to cellular features and to architectural aspects, employing MPT/FLIM, and to establish the terminology for their assessment. To this purpose, we evaluated the presence and the frequency of the descriptors in two test sets of images, comprising melanocytic nevi and a miscellaneous population. MPT/FLIM descriptors of melanocytic nevi were compared with RCM and histopathological findings.

Materials and Methods

Study design

The study was divided into two parts, a preliminary study and a main study. In the former, MPT/FLIM images referring to 16 *ex vivo* nevi were simultaneously evaluated by three observers (SS, FA, and MM) for the identification of morphological descriptors characteristic of melanocytic nevi. Proposed descriptors were discussed and the parameters referring to epidermal keratinocytes, epidermal melanocytes, dermo-epidermal junction, papillary dermis and lesion architecture were selected after unanimous approval.

In the main study, the presence/absence of the specified criteria were blindly evaluated on a test set, comprising 102 *ex vivo* samples (51 melanocytic nevi and 51 miscellaneous skin lesions) by two independent observers (SS, SB), who also classified the images into those pertaining to melanocytic nevi or 'other'. Fluorescence lifetime values inside a region of interest corresponding to three cells per sample were calculated on images acquired by an excitation wavelength of 760 nm on 48 healthy skin and 48 melanocytic nevus samples.

Lesions and patients

The MPT/FLIM images of 67 melanocytic nevi, which were excised because of equivocal dermoscopic aspects, were evaluated. All lesions

underwent conventional histhopathological examination. Considering only the 51 lesions constituting the test set, 40 lesions were histologically defined as compound nevi, 6 as junctional nevi, and 5 as dermal nevi. Thirty-five lesions were localized on the trunk, 11 on the limbs, and 5 on the face and the scalp. These 51 lesions were surgically removed from 49 patients (30 men and 19 women), whose age ranged from 19 to 88 years.

The miscellaneous population comprised of 51 histologically confirmed lesions, including 18 basal cell carcinomas, 13 squamous cell carcinomas, 7 dermatofibromas, 5 actinic keratosis, 2 seborrheic keratosis, 1 condrodermatitis, 1 atypical fibroxantoma, 1 leyomiosarcoma, 1 lentigo simplex, 1 neurofibroma and 1 desmoplastic trichoepithelioma.

Instrumentation and elaboration of the data

Multiphoton laser tomography

In this study, we used the MPT DermaInspect® imaging system (Jenlab GmbH, Jena, Germany) that provides intratissue scanning with subcellular spatial resolution (0.5 μm in lateral direction and 1–2 μm in the axial direction) (8, 17–20). This CE-marked and commercially available imaging tool is rated as a class 1M device according to the European laser safety regulations and consists of three major modules: excitation laser, scanning unit and control module. The laser source utilizes a mode-locked, 80 MHz, Ti:Sapphire laser (Mai-Tai; Spectra Physics, Mountain View, CA, USA) with a tuning range of 710–920 nm, a 75 fs pulse width and a maximum laser power of 900 mW that is attenuated to a maximum of 50 mW at the sample. The scanning unit includes a beam expander, fast $x-y$ galvoscanners, a 40× focusing objective (NA = 1.3 oil), a time-correlated single photon counting (TCSPC) module for FLIM and a photomultiplier tube (PMT) for intensity imaging. A colour-glass filter (Schott BG39) is employed in front of the PMT to block the scattered laser radiation light.

Fluorescence lifetime imaging

Fluorescence lifetime imaging was implemented in the DermaInspect® system using a time-correlated single photon counting (TCSPC) module with a temporal instrument response function of approximately 250 ps (full-width at half-maximum). The emitted autofluorescence was spectrally selected by means of a short pass optical filter (Schott BG39) to protect the detector (PMH 100-1; Becker & Hickl GmbH, Berlin, Germany) from scattered excitation light. The TCSPC data were processed using SPCImage (Becker & Hickl GmbH). The raw TCSPC images were smoothed using a 5 × 5 kernel (SPCImage binning set to 2) and a single exponential decay fitting model was employed to obtain an estimate of the mean fluorescence lifetime at each pixel. The final output of the FLIM analysis is a pseudocolour image where the colour scale encodes the fluorescence lifetime and image brightness encodes the fluorescence intensity. False-colour lifetime maps of *ex vivo* samples were produced by assigning a colour according to its lifetime value to each pixel of the image. All images were displayed with a fluorescence lifetime range from red (0 ps) to blue (2000 ps).

Image acquisition and analysis

Ex vivo samples were placed on a cork disc covered by a transparent film and a gauze. For the examination of the samples a drop of water was placed between the skin and the cover glass, which was then attached to a metal coupling ring by circular adhesive tape. The metal coupler was magnetically connected to the MPT system after applying a drop of oil (Immersol 518F; Carl Zeiss Ltd, Standort Gottingen-Vertrieb, Gottingen, Germany) between the cover glass and the objective. The surface of the skin was found by using a coarse manual adjustment of the focus. Following this, a specific layer was selected by fine adjustment of the focus via a piezo positioner controlled by the software JLScan 1100. The imaging depth was first pinpointed to the upper layer (stratum corneum); for the acquisition of stacks, a stepwise descent from the surface to a depth of approximately 200 μm was then performed with an interval of 15 μm. The maximum imaging depth corresponds to the working distance of the focusing optics of the DermaInspect® system (200 μm). One optical section, consisting of 256 × 256 pixels, was taken with a scanning time of 25.5 s/frame and an excitation power between 20 and 45 mW.

For the evaluation of epidermal structures we used an excitation wavelength of 760 nm to

preferentially excite intracellular NADH in the stratum corneum and the keratinocytes. Switching the excitation wavelength to 800 nm provided preferential excitation of melanin, in particular in pigmented keratinocytes and melanocytes in the basal layer and at the junction surrounding the papillae. Increasing the wavelength to 820 nm generated two types of signal in dermal fibres: autofluorescence from both collagen fibres and elastin fibres and second harmonic generation in collagen fibres. Separation of these signals was accomplished by utilizing a long pass optical filter (Semrock, BLP01-405R-25, 0.04% transmission at 415 nm) that can be inserted into the beam path and which excludes the SHG component of the signal when exciting with wavelengths up to 820 nm. FLIM data produced by SPCImage were analysed using a custom-written software package ('FLIM analysis assistant software') provided by the Photonics Group at Imperial College London, to calculate the mean fluorescence intensity and lifetime values for selected areas of interest such as the cytoplasm of single cells.

Imaging of the samples

Each sample was excised during dermatological surgery, then cut, saving some healthy skin, to obtain a regular shape, thereby facilitating its positioning under the microscope. The tissue specimens excised contained the entire skin lesion and normal perilesional skin from the ends of the spindle-shaped resection. For observation, saline solution was used as the immersion medium under the objective lens to maintain the natural tissue osmolarity. Two-dimensional, horizontal images were acquired through optical sectioning parallel to the tissue surface (i.e. in the $x-y$ plane). Three-dimensional data sets, called z-stacks, were obtained by sequentially changing the plane of focus (z-level), thus scanning at different tissue depths. Imaging was accomplished within 30 min from biopsy.

All images analysis was performed using pseudocolour FLIM images produced by the SPCImage software. For each sample of the test set, 15 FLIM stacks were examined. In total, 765 images of nevi and an equivalent number of other skin lesion samples were considered. For the evaluation of the lesions, a 0–2000 ps colour scale was employed.

The local ethics committee granted approval of the study protocol before the start of the study.

Statistics

The frequency of each descriptor in melanocytic nevi and other skin lesions was computed, and the chi-squared test and the Fisher's exact test were calculated. Sensitivity and specificity values of single descriptors and of the MPT/FLIM diagnosis of nevus were evaluated as compared with histopathological diagnosis. The agreement between ratings made by two observers on the diagnosis of nevus and on specific patterns (inter-rater reliability) was estimated using the Cohen's kappa statistics with 95% confidence intervals. Finally, mean values and standard deviations of the fluorescence decay in healthy and nevus cells were calculated and differences were assessed by means of the Student's t-test. A P-value <0.05 was considered statistically significant. Statistical examinations were performed with SPSS 19.0 for Windows (SPSS Inc., Chicago, IL, USA).

Results

Preliminary study

Normal perilesional skin

The morphological features as observed by FLIM in the specimens of normal perilesional skin were similar to those already reported (21). Keratinocytes exhibit an intermediate fluorescence lifetime which was calculated on 48 healthy skin samples: the average lifetime value was 1000 ps with a standard deviation of 200 ps. Epidermal keratinocytes appear green according to our 0–2000 ps colour scale, whereas cells or structures with a shorter fluorescence lifetime (coded red) correspond to melanocytes or pigmented keratinocytes and melanosomes respectively.

Melanocytic nevi

After evaluation of 240 images corresponding to the depth stacks of 16 melanocytic nevus samples, we identified 13 descriptors referring to epidermal keratinocytes and melanocytes, dermo-epidermal junction, papillary dermis and overall architecture.

Epidermis. 'Short-lifetime cells in the stratum corneum' appear as cells of different size, sometimes displaying more than one nucleus and

speckled melanin (Fig. 1a,b). 'Melanin-containing keratinocytes' are recognizable in FLIM images as keratinocytes-containing spots or patches with a short fluorescence lifetime of less than 450 ps, (red to yellow in the 0–2000 ps pseudocolour scale) characterizing melanin (17). The melanin blotch inside the keratinocyte may be unique, involving a large part of the

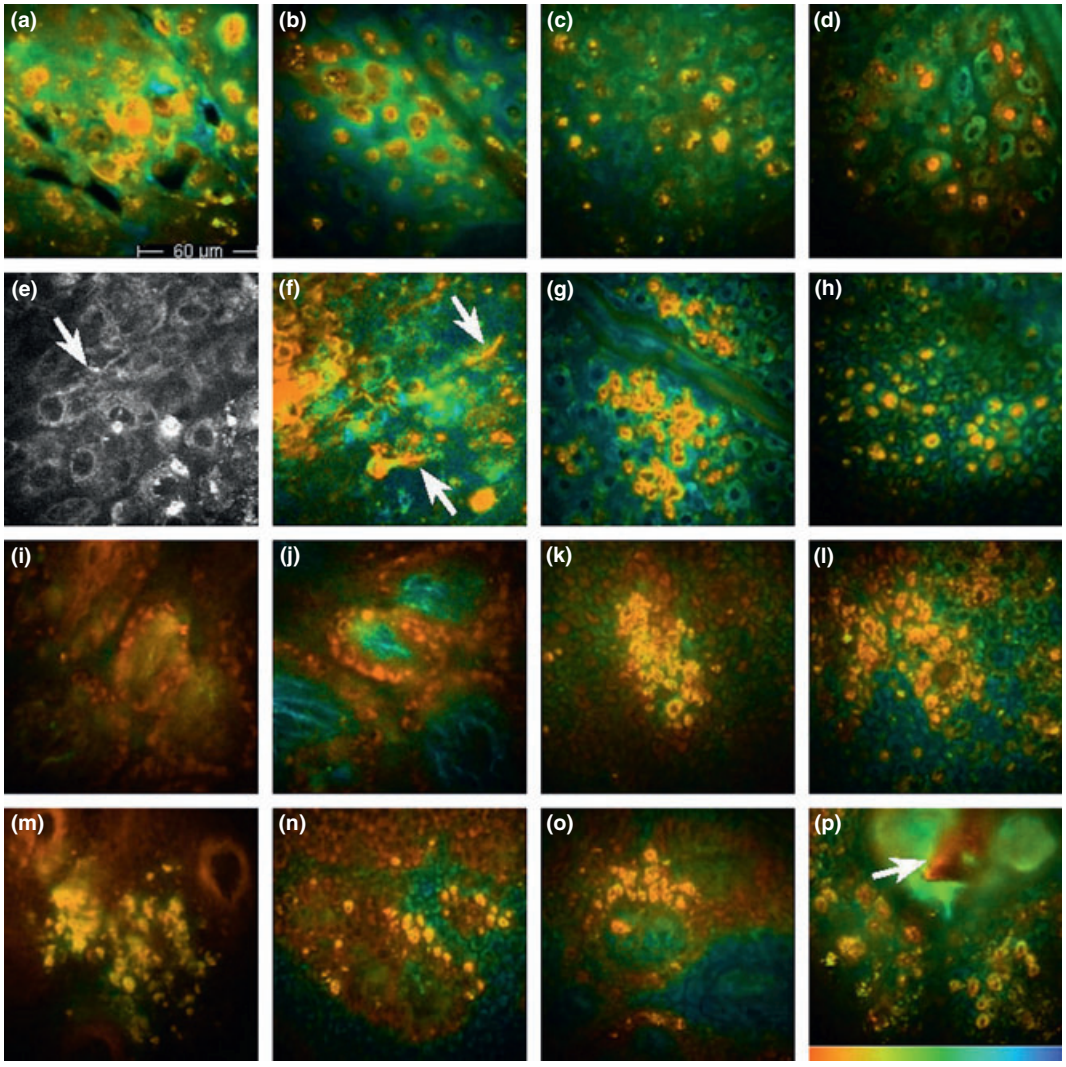

Fig. 1. (a, b) 760 nm excitation wavelength; 0–2000 ps pseudocolour scale; 10 m depth (a), 15 m depth (b). 'Short-lifetime cells in the stratum corneum' are well visible appearing large, different in size and shape with speckled melanin inside. (c, d) 760 nm excitation wavelength; 0–2000 ps pseudocolor scale; 20 m depth. Going deeper from the stratum corneum, we find 'melanin-containing keratinocytes'; the pigment can involve all the cytoplasm sparing the nucleus or can be organized in blotches. (e) 760 nm excitation wavelength; autofluorescence image; 70 m depth. 'Dendritic cells' with thin and fluorescent (white) branches raising from the cellular body (arrow). (f) 760 nm excitation wavelength; 0–2000 ps pseudocolour scale; 75 m depth. Short lifetime 'dendritic cells' appearing orange (arrows). (g) 760 nm excitation wavelength; 0–2000 ps pseudocolour scale; 20 m depth. 'Small short-lifetime cells', smaller than keratinocytes in the upper epidermal layers. (h) 760 nm excitation wavelength; 0–2000 ps pseudocolour scale; 45 μm depth. 'Small short-lifetime cells' whose size doesn't differ from keratinocytes' of the lower layers. (i) 800 nm excitation wavelength; 0–2000 ps pseudocolour scale; 80 m depth. Increasing the excitation wavelength 'edged papillae' constituted by a rim of short-lifetime cells surrounding an oval space with collagen fibres are visible. (j) 820 nm excitation wavelength; 0–2000 ps pseudocolour scale; 90 m depth; long-pass filter excluding SHG signal. Only elastic fibres in the papillae, appearing blue according to their long fluorescence lifetime, are observable. (k, l) 760 nm excitation wavelength; 0–2000 ps pseudocolour scale; 70 m depth (k); 40 m depth (l). 'Junctional nests of short-lifetime cells' at the dermo-epidermal junction, constituted by yellow-orange cells according to their melanocytic nature (short fluorescence lifetime). (m) 820 nm excitation wavelength, 0–2000 ps pseudocolour scale, 110 m depth. 'Dermal cell clusters' in the papillary dermis developing into the interpapillary spaces. (n) 760 nm excitation wavelength; 0–2000 ps pseudocolour scale; 40 m depth. Isolated cells bulging from the papillae, arising from their boundaries. (o, p) 760 nm excitation wavelength; 0–2000 ps pseudocolour scale; 60 m depth (o); 50 m depth (p). 'Short lifetime cells in the papilla' corresponding to melanophages or inflammatory cells; hair follicle (arrow); 0–2000 ps pseudocolour scale.

cytoplasm and sparing the nucleus, or it may be organized in multiple spots, conferring a granular appearance to the keratinocyte (Fig. 1c,d). Sometimes the melanin blotch is disposed to form a cap over the nucleus, which is not recognizable because of the horizontal optical section of the sample.

We also observed 'dendritic cells', which correspond to cells with branching ramifications and dendrites (Fig. 1e,f). When the presence of only one or two of them was recorded, they were defined as 'sporadic dendritic cells'.

Epidermal melanocytes in the upper and the lower layers, defined as 'small short-lifetime cells' appear as tiny cells, which are smaller than keratinocytes and show a well-visible small nucleus and homogeneously distributed melanin (Fig. 1g,h).

Dermo-epidermal junction. At the level of the dermo-epidermal junction the tips of the dermal papillae, appearing as roundish structures surrounded by a regular orange boundary made up of keratinocytes and melanocytes, are visible. 'Edged papillae' are characterized by a well-demarcated rim of orange cells surrounding a dark space containing fibres or cells (Fig. 1i,j), whereas 'non-edged papillae' lack a well-defined boundary. The dermal papillae were not always visible, and this is probably due to a thicker epidermal layer in these specimens and the limited imaging depth, and to the lesion morphology, when nodular.

Nevus cells forming aggregates of melanocytes appearing as bulges rising from the periphery of the papillae were defined 'junctional nests of short-lifetime cells'. They are well correlated with the histological finding of melanocytic nests in junctional and compound nevi (Fig. 1k,l).

Papillary dermis. Exploring the superficial or papillary dermis bright 'dermal cell clusters' or isolated cells bulging from the papillae are visible (Fig. 1m,n); they arise from the papillary contour and develop into the interpapillary spaces. Because of their marked fluorescence, they are well visualized with MPT, and it is easy to distinguish them from keratinocytes. Their short-lifetime value, corresponding to yellow on the 0–2000 ps colour scale, confirms their melanocytic nature.

In the papillary dermis we can also find 'short-lifetime cells in the papilla' (Fig. 1o,p). They are generally isolated or grouped into small clusters, and are bigger than melanocytes. Thanks to their brightness, they are well visible inside the papillae intermingled with collagen and elastic fibres. It is reasonable to identify them as melanophages.

Architecture. Epidermal layers and the dermo-epidermal junction may show a 'monomorphic and regular histoarchitecture' or an 'architectural disarray'. These descriptors contribute to the assessment of the benignity of the lesion.

Main study

Frequency of epidermal and melanocytic nevi descriptors

The frequency of the descriptors in nevi and in the control population is illustrated in Table 1. We can appreciate that 'small short-lifetime cells upper layers' and 'small short-lifetime cells lower layers' are found in almost all melanocytic nevi. In fact they were present in 98% of melanocytic lesions, whereas their frequency in the control population was 1.9% and 17.6% for upper and lower layers respectively. 'Dendritic cells' in the control population were never

TABLE 1. Frequency of FLIM descriptors in melanocytic nevi and control population, Chi-squared test and Fisher's exact test, sensitivity and specificity values, interobserver agreement (Kappa values)

FLIM descriptors	Melanocytic nevi 51 (100%)	Control population 51 (100%)	χ^2 (significance)	Fisher's exact test	Sensitivity	Specificity	K values (significance)
Small short-lifetime cells upper layers	50 (98)	1 (1.9)	86.761 (0.000)	0.000	98.03	98.04	0.485 (0.000)
Small short-lifetime cells lower layers	50 (98)	9 (17.6)	57.177 (0.000)	0.000	98.03	82.35	0.381 (0.000)
Dendritic cells	4 (7.8)	0	4.163 (0.041)	0.118	7.84	100	1 (0.000)
Edged papillae	42 (82.3)	4 (7.8)	62.963 (0.000)	0.000	82.35	92.16	0.704 (0.000)
Junctional nests of short-lifetime cells	48 (94.1)	0	87.164 (0.000)	0.000	94.11	100	0.847 (0.000)
Dermal cell clusters	29 (56.8)	2 (3.9)	24.984 (0.000)	0.000	56.86	96.08	0.728 (0.000)
Diagnosis of melanocytic nevus	51 (100)	0	102.000 (0.000)	0.000	100	100	1 (0.000)
Aligned elongated cells	0	15 (29.4)	17.586 (0.000)	0.000	0	70.59	Not applicable
Double alignment	0	3 (5.8)	3.091 (0.079)	0.243	0	94.12	Not applicable
Phantom islands	0	7 (13.7)	7.516 (0.006)	0.013	0	86.27	Not applicable

found, whereas they were observed in four nevi (7.8%). 'Edged papillae' were found in 82.3% of melanocytic nevi, whereas in control lesions their frequency was 7.8%. The control population did not show the presence of 'junctional nests of short-lifetime cells', which can be considered one of the most representative descriptors of melanocytic nevi, being present in 94.1% of nevi. Finally, 'dermal cell clusters' were present in 56.8% of melanocytic nevi and in 3.9% of the miscellaneous population.

As shown in Table 1, it was always possible to correctly diagnose melanocytic nevi, whereas lesions belonging to the control population were never defined as 'melanocytic nevi'.

No BCC descriptors, i.e. aligned elongated cells, double alignment and phantom island (11, 12) were observed in our nevi population.

Table 1 also lists values referring to sensitivity and specificity for the diagnosis of melanocytic nevus and of single descriptors. The diagnosis of melanocytic nevus showed 100% sensitivity and specificity. 'Dendritic cells' was the descriptor with the lower sensitivity (7.84%), but with a 100% specificity. 'Small short-lifetime cells' in the upper and lower layers, 'edged papillae' and 'junctional nests of short-lifetime cells' had a high sensitivity and specificity; in particular, 'junctional nests' showed a 100% specificity. 'Dermal cell clusters' exhibited a low sensitivity (47.06%) but a high specificity (96.08%).

Interobserver agreement was also calculated. Kappa values ranged from 0.381 to 1 and were significant for each descriptor. In particular, 'dendritic cells' and diagnosis of melanocytic nevus showed the maximum interobserver reliability value. Also 'junctional nests of short-lifetime cells' and 'dermal cell clusters' exhibited a high Kappa value of 0.847 and 0.728 respectively.

Significant differences between nevi and other lesions were observed for all melanocytic nevus descriptors. BCC descriptors were never found in nevi; since their frequency was also low in the control population which included only 18 BCCs, specificity ranged from 70.59% to 94.12%. For the same reason, the difference for the 'double alignment' descriptor was not significant. Table 2 reports the data referring to the different histological nevus subtypes.

TABLE 2. Frequency of the descriptors in different histological nevus subtypes

	Junctional 6 (100%)	Compound 40 (100%)	Dermal 5 (100%)
Epidermis			
Short-lifetime cells in the stratum corneum	1 (16.6)	14 (35)	0
Large cells	1 (16.6)	13 (32.5)	0
Polyinucleated cells	1 (16.6)	10 (25)	0
Speckled melanin	1 (16.6)	12 (30)	0
Cells with different size	1 (16.6)	14 (35)	0
Melanin-containing keratinocytes	6 (100)	37 (92.5)	5 (100)
Sporadic dendritic cells	0	3 (7.5)	0
Dendritic cells	0	1 (2.5)	0
Small short-lifetime cells upper layers	6 (100)	39 (97.5)	5 (100)
Small short-lifetime cells lower layers	6 (100)	39 (97.5)	5 (100)
Dermo-epidermal junction			
Edged papillae	6 (100)	35 (87.5)	1 (20)
Non-edged papillae	0	12 (30)	0
Junctional nests of short-lifetime cells	6 (100)	40 (100)	2 (40)
Papillary dermis			
Dermal cell clusters	0	29 (72.5)	0
Short-lifetime cells in the papilla	2 (33.3)	18 (45)	0
Architecture			
Monomorphic and regular histo architecture	6 (100)	29 (72.5)	5 (100)
Architectural disarray	0	11 (27.5)	0

Epidermis

'Short-lifetime cells in the stratum corneum', large, inhomogeneous in size, polynucleated and with speckled melanin, were found in 16.6% of junctional nevi and in 35% of compound nevi. The presence of 'melanin-containing keratinocytes' was found in the totality of junctional and dermal nevi and in 92.5% of compound nevi. Dendritic cells were never found in junctional and dermal nevi, whereas they were observed in four compound nevi. Small melanocytic cells, described as 'small short-lifetime cells upper and lower layers' were found in all junctional and dermal nevi and in 97.5% of compound nevi.

Dermo-epidermal junction

All junctional nevi exhibited 'edged papillae', whereas compound nevi showed them in 87.5% of the cases and dermal nevi in one case. Thirty per cent of compound nevi were characterized by the presence of 'non-edged papillae'. 'Junctional nests of short-lifetime cells' were observed in all junctional and compound nevi and in 40% of dermal nevi.

Papillary dermis

'Dermal cell clusters' were only observable in 72.5% of compound nevi, probably due to the decreasing laser power when deepening into

the dermis, especially when observing thick lesions. This descriptor was also never visible in junctional nevi, where the melanocytic component only involves the dermo-epidermal junction. 'Short-lifetime cells in the papilla' were observed in 45% of compound nevi and in 33.3% of junctional nevi; they were never found in dermal nevi.

Architecture

All junctional and dermal nevi and also 72.5% of compound nevi showed a 'monomorphic and regular histoarchitecture' with regular papillae and no evidence of atypical cells or random organization and disarrangement of the epidermal layers. None of the junctional and dermal nevi showed an 'architectural disarray', which was detected in 27.5% of compound nevi.

The mean fluorescence lifetime value of 48 nevi, calculated on three representative cells for each sample, was 360 ps with a standard deviation value of 120 ps, corresponding to the red-orange-yellow colour (significantly different from the lifetime values of keratinocytes).

Discussion

Non-invasive imaging techniques have been introduced to help the clinician in the early identification of malignant and suspicious lesions. Dermoscopy represents an efficient diagnostic tool allowing the evaluation of skin structures located under the skin surface (2, 3). Confocal microscopy enables an *in vivo* non-invasive visualization of skin structures at a very high resolution, near to the histopathological one (4). The observation of dermoscopic and confocal features in melanocytic lesions examined by histology allowed the correlation between morphological and histological features and the building up of a 'common language' for expert users (5, 7).

Multiphoton laser tomography has been recently introduced as a non-invasive diagnostic tool enabling the assessment of the skin with a subcellular resolution with a great potential both in research fields and in clinical practice (9, 10). This imaging modality relies on the simultaneous excitation of endogenous fluorophores by two or more photons of low energy in the NIR spectrum wavelength (10). Since its introduction, it has contributed to progress in biology and medicine, especially for the characterization and quantification of physiological or pathological skin features and for the dynamic analysis of subtle cutaneous changes, avoiding biopsy procedures and fixation, sectioning and staining for histological examination (10). The MPT has allowed the study of healthy skin, photoaging, melanocytic lesions and epithelial tumours. In particular, it has been extensively employed for the definition of BCC features *in vivo* and *ex vivo* (11); thanks to the possibility to combine FLIM to MPT, several morphological BCC descriptors (such as phantom islands, aligned elongated cells and double alignment) have been identified by our group enabling its differentiation from healthy skin and other skin lesions (12, 13).

In this study, we aimed at identifying MPT/FLIM features of melanocytic nevi, possibly characterizing different nevus subtypes and at establishing a reproducible terminology for the description of these lesions. To meet these aims, a population of dermoscopically suspicious but histologically benign melanocytic nevi was examined and compared with a control population of miscellaneous lesions. We identified five sensitive and specific descriptors for melanocytic nevi, i.e. small short-lifetime cells in the upper and lower epidermal layers, edged papillae, junctional nests of short-lifetime cells and dermal cell clusters. As criteria useful for differential diagnosis between benign nevi and malignant melanoma, Dimitrow et al. considered the presence of a monomorphic and regular histoarchitecture, evenly distributed keratinocytes, well-defined cell borders and rarely seen dendritic cells (16). The high frequency of these aspects in benign melanocytic nevi was also confirmed by our study; in particular, a monomorphic and regular histoarchitecture was observed in 40/51 nevi and dendritic cells were found only in 4/51 nevi. On the other hand, BCC descriptors were never found in nevi, and, starting the examination of a melanocytic lesion, the differences from healthy skin and BCCs are extremely clear at the first glance: melanocytic aggregates and absence of basaloid nests and long lifetime 'blue' cells enable us to immediately exclude the diagnosis of BCC.

When imaging only with MPT, skin keratinocytes and melanocytes are not distinguishable on a morphological basis with certainty, nor is intrakeratinocytic melanin evident. In the MPT

intensity image, melanin-containing cells and melanin appear as hyperintense fluorescent cells and bright clusters, respectively, at 800 nm (8, 17) due to the preferential excitation of melanin compared with NAD(P)H at this wavelength (17, 22). To identify the presence of melanin in the skin with a higher level of confidence, the fluorescence decay time can be imaged. In our MPT/FLIM images, represented by a 0–2000 ps colour scale, keratinocytes, which have a fluorescence decay time around 1000 ps, appear green, whereas melanin, with its short fluorescence decay time, corresponds to red-orange hues.

Melanin-containing keratinocytes, recognizable for the presence of short-lifetime patches inside the cytoplasm, and melanocytes, appearing as small uniformly 'red-coloured' cells with a small nucleus, were visible in the majority of nevi. In one-third of compound nevi, large short-lifetime cells, sometimes polynucleated and with speckled melanin, were also visible in the stratum corneum. Junctional melanocytic nests appeared as aggregates of short-lifetime cells in continuity with those surrounding the papillae, whereas dermal nests corresponded to dermal clusters of short-lifetime cells. All of these short-lifetime 'red' cells were well distinguishable from 'green' (1000 ps) keratinocytes, 'blue' (long lifetime) keratinocytes surrounding hair follicles, 'red' collagen fibres and 'blue' elastin fibres. The MPT/FLIM also enabled the description of the different histological subtypes of nevi.

Histologically, junctional nevi are characterized by a proliferation of single cells or the presence of small nests at the junction. Under RCM, junctional nevi show the so-called ringed pattern, with regular edged papillae formed by regularly sized and shaped bright cells, surrounding dark oval spaces (dermal papillae); the correspondent MPT/FLIM descriptor corresponds to edged papillae, which were found in the totality of the samples. In two of six cases, we also noticed the presence of short-lifetime cells within the papillae; these may be interpreted as inflammatory cells (melanophages, lymphocytes), mentioned in the histopathology reports. It is also well known that confocal microscopy is able to visualize plump bright cells, with faded borders, within the dermal papillae, with the meaning of inflammatory cells.

Histopathology shows that the compound nevus subtype has a junctional and a dermal component involving the superficial or the deep dermis. Under MPT/FLIM, compound nevi are characterized by the presence of melanin-containing keratinocytes, and small short-lifetime cells in the upper and lower epidermal layers. In the majority of compound nevi we found the presence of edged papillae and in only four cases it was possible to observe dendritic cells in the epidermal layers. By histological examination discrete nests of melanocytes/nevus cells are found at the dermo-epidermal junction, usually located on the rete ridges. Corresponding RCM features of compound nevi are interpapillary thickening and dense junctional nests bulging within the dermal papillae, or the presence of dense, well demarcated and reflectant nests in the upper dermis. In all compound nevi assessed by MPT/FLIM, we observed short-lifetime cell nests at the dermo-epidermal junction. These nests can sometimes bulge into the underlying dermis which may contain a few melanophages and a lymphohistiocytic infiltrate, corresponding to our observations of dermal cell clusters and short-lifetime cells in the papillae. The inflammatory component is also well visible by RCM, where a variable amount of single plump bright cells within the dermis can be observed.

Intradermal nevi include nevi with melanocytic cells only localized in the dermis. Nevus cells are mostly arranged forming nests and cords. Sometimes, in the deeper part of the lesions, the nevus cells may assume a neuroid appearance (23). Also under confocal, these nevi reveal absence of specific features in the upper layers and at the junction, and dense and dense/sparse nests in the dermis. Under MPT/FLIM we always noticed the presence of melanin-containing keratinocytes and small short-lifetime cells in the upper and lower epidermal layers. In some cases we also observed the presence of junctional nests of short-lifetime cells at the dermo-epidermal junction. However, dermal cell clusters were never visible due to the limited penetration depth of our MPT system and the increased epidermal thickness in dome-shaped dermal nevi.

In conclusion, we have identified specific and sensitive MPT/FLIM descriptors for benign melanocytic lesions, matching with those already detected by RCM and corresponding to histopathological findings, on *ex vivo* samples.

Compared with confocal microscopy, the DermaInspect® has a smaller field of view

(350 × 350 μm). On the other hand, MPT/FLIM, allows the excitation of endogenous fluorophores and has a higher resolution (0.5 μm in the horizontal plane, and 1–2 μm in the axial direction), enabling the identification of subcellular structures. By RCM, melanin-containing keratinocytes and melanocytes cannot be distinguished; they both appear as bright, roundish to polygonal monomorphic cells, usually small, located at the basal layer and at the DE junction. On the contrary, FLIM, particularly due to its ability to identify melanin by its short fluorescence lifetime, provides a clue for the identification of melanocytes in the skin. For these reasons MPT/FLIM represents a breakthrough with respect to other imaging techniques and it is desirable that it will be introduced in clinical practice for the identification of melanocytic lesions and their differentiation from epithelial cancer.

Acknowledgements

The authors would like to thank Marcel Höfer of JenLab for his expert technical assistance. The study was supported by the European Communities (grant agreement no. HEALTH-f7-2008-201577).

Conflicts of Interest

Karsten König is the CEO of Jenlab.

References

1. Seidenari S, Longo C, Giusti F, Pellacani G. Clinical selection of melanocytic lesions for dermoscopy decreases the identification of suspicious lesions in comparison with dermoscopy without clinical preselection. Br J Dermatol 2006; 154: 873–879.
2. Pehamberger H, Steiner A, Wolff K. *In vivo* epiluminescence microscopy of pigmented skin lesions. I. Pattern analysis of pigmented skin lesions. J Am Acad Dermatol 1987; 17: 571–583.
3. Soyer HP, Argenziano G, Talamini R, Chimenti S. Is dermoscopy useful for the diagnosis of melanoma? Arch Dermatol 2001; 137: 1361–1363.
4. Rajadhyaksha M, Grossman M, Esterowitz D, Webb RH, Anderson RR. *In vivo* confocal scanning laser microscopy of human skin: melanin provides strong contrast. J Invest Dermatol 1995; 104: 946–952.
5. Scope A, Benvenuto-Andrade C, Agero AL et al. *In vivo* reflectance confocal microscopy imaging of melanocytic skin lesions: consensus terminology glossary and illustrative images. J Am Acad Dermatol 2007; 57:644–658. Epub 2007 Jul 16.
6. Bassoli S, Ahlgrimm-Siess , Casari A, Pellacani G. Common nevi. In: Hofmann-Wellenhof R, Pellacani G, Malvehy J and Soyer HP, eds. Reflectance confocal microscopy for skin diseases. Berlin, Heidelberg: Springer-Verlag; 2012; 8: 73–86.
7. Pellacani G, Longo C, Malvehy J, Puig S, Carrera C, Segura S, Bassoli S, Seidenari S. *In vivo* confocal microscopic and histopathologic correlations of dermoscopic features in 202 melanocytic lesions. Arch Dermatol 2008; 144: 1597–1608.
8. Riemann I, Dimitrow E, Fischer P, Reif A, Kaatz M, Elsner P, König K. High resolution multiphoton tomography of human skin *in vivo* and *in vitro*. SPIE-Proceeding 2004; 5312: 21–28.
9. Lin SJ, Jee SH, Dong CY. Multiphoton microscopy: a new paradigm in dermatological imaging. Eur J Dermatol 2007; 17: 361–366.
10. Tsai TH, Jee SH, Dong CY, Lin SJ. Multiphoton microscopy in dermatological imaging. J Dermatol Sci 2009; 56: 1–8.
11. Seidenari S, Arginelli F, Bassoli S et al. Diagnosis of BCC by multiphoton laser tomography. Skin Res Technol. 2012; doi: 10.1111/j.1600-846.2012.00643.x. [Epub ahead of print].
12. Seidenari S, Arginelli F, French P, König K, Magnoni C, Manfredini M, Ponti G, Talbot C, Dunsby C. Multiphoton laser tomography and fluorescence lifetime imaging of basal cell carcinoma: morphologic features for non-invasive diagnostics. Exp Dermatol. 2012; 21: 831–836.
13. Manfredini M, Arginelli F, Dunsby C, French PMW, Talbot C, K nig K, Pellacani G, Ponti G, Seidenari S. High-resolution imaging of basal cell carcinoma: a comparison between multiphoton microscopy with fluorescence lifetime imaging and reflectance confocal microscopy. Skin Res Technol 2012. doi: 10.1111/j.1600-0846.2012.00661.x. [Epub ahead of print]
14. Cicchi R, Massi D, Sestini S, Carli P, De Giorgi V, Lotti T, Pavone FS. Multidimensional non-linear laser imaging of basal cell carcinoma. Opt Express 2007; 15: 10135–10148.
15. Patalay R, Talbot C, Alexandrov Y et al. Multiphoton multispectral fluorescence lifetime tomography for the evaluation of basal cell carcinomas. PLoS One 2012; 7: e43460.
16. Dimitrow E, Ziemer M, Koehler MJ, Norgauer J, König K, Elsner P, Kaatz M. Sensitivity and specificity of multiphoton laser tomography for *in vivo* and ex vivo diagnosis of malignant melanoma. J Invest Dermatol 2009; 129: 1752–1758.
17. Dimitrow E, Riemann I, Ehlers A, Koehler MJ, Norgauer J, Elsner P, König K, Kaatz M. Spectral fluorescence lifetime detection and selective melanin imaging by multiphoton laser tomography for melanoma diagnosis. Exp Dermatol 2009; 18: 509–515.
18. Kollias N, Zonios G, Stamatas GN. Fluorescence spectroscopy of skin. Vib Spectrosc 2002; 28: 17–23.
19. König K, Riemann I. High-resolution multiphoton tomography of human skin with subcellular spatial resolution and picosecond time resolution. J Biomed Opt 2003; 8: 432–439.
20. Schenke-Layland K, Riemann I, Damour O, Stock UA, König K. Two-photon microscopes and *in vivo* multiphoton tomographs-powerful diagnostic tools for tissue engineering and drug delivery. Adv Drug Deliv Rev 2006; 58: 878–896.

21. Benati E, Bellini V, Borsari S et al. Quantitative evaluation of healthy epidermis by means of multiphoton microscopy and FLIM. Skin Res Technol 2011; 17: 295–303.
22. Teuchner K, Ehlert J, Freyer W, Leupold D, Altmeyer P, Stucker M, Hoffmann K. Fluorescence studies of melanin by stepwise two-photon femtosecond laser excitation. J Fluoresc 2000; 10: 275–281.
23. Weedon D. Lentigines, nevi, and melanomas. In: Weedon D, ed. Skin pathology. Edinburgh, Scotland: Churchill-Livingston 1997: 673–711.

Address:
Federica Arginelli
Department of Dermatology
Via del Pozzo 71
41124 Modena
Italy
Tel: +39594222924
Fax: +39594224271
e-mail: federica.arginelli@libero.it